EVALUATION OF THE BARK BEETLE GREEN ATTACK DETECTABILITY IN SPRUCE FOREST FROM MULTITEMPORAL MULTISPECTRAL UAV IMAGERY

Salma Bijou[1], Lucie Kupková[1], Markéta Potůčková[1], Lucie Červená[1], Jakub Lysák[1]

[1] Department of Applied Geoinformatics and Cartography, Faculty of Science, Charles University, Albertov 6, Prague 2, Czech Republic - (salma.bijou, lucie.kupkova , marketa.potuckova, lucie.cervena, jakub.lysak)@natur.cuni.cz

KEY WORDS: Green Attack, UAV, Multispectral, Bark Beetle, Norway spruce

ABSTRACT:

Forests have always been a major concern for public authorities given their significant role as a resource for timber production, as well as for climate regulation. The infestation of bark beetles poses a challenging problem in forests, causing tree mortality, reduced timber quality, and ecosystem disruption. Multispectral imagery (MS) captured from unmanned aerial vehicles (UAVs) are increasingly employed for forest health assessment and have been extensively used to map the tree mortality caused by bark beetles. However, its utilisation for the identification of the initial stage of infestation known as "green attack" when infested trees do not display any visible symptoms yet, is still uncertain. This study is innovative in the ways it works with so far rare dense and comprehensive time series of MS UAV imagery starting in the initial month prior to the infestation and before the development of the Bark Beetle (BB) infestation visual symptoms, aiming to evaluate the detectability of bark beetle (Ips typographus L.) green attack. The study area predominantly covered by Norway spruce (Picea abies (L.) Karst.) is located in the Krkonoše Mountains National Park, in the Czech Republic. From May to August 2022, a total of nine MS UAV datasets were acquired with a DJI Phantom 4 MS sensor. The research question is whether infested trees exhibit significantly different changes in the spectra compared to healthy trees at an early stage. The detectability of green attacks was statistically investigated along with the underlying factors (flowering, growth of new shoots) that can affect the accuracy of detection. The results showed a distinct reduction in tree vitality of the infested trees in the late summer season and later stages of infestations. Based on our findings, we conclude that the proposed methods using UAV MS images can be employed to map local infestations and evaluate the tree vitality throughout the season, but the early detection of the green attack stage (in the absence of visible symptoms at the crown level) of Bark Beetle infestation from UAV MS data remains unfeasible. The precision of the detection using statistical methods can be further investigated using a time series of UAV hyperspectral images that offer a higher spectral resolution.

1. INTRODUCTION

Forests worldwide are being impacted by climate change. Coniferous forests in Central Europe are experiencing pest attacks which may be related to the weakening of forest ecosystems due to drought and could endanger the stability of forest stands. In the Czech Republic, there has been a noteworthy increase in salvage cutting over the past five years due to the infestation of trees with the European spruce bark beetle, also known as the Bark Beetle (Ips typographus L.). This has resulted in significant economic and ecological losses, with 32 million cubic meters of raw wood harvested from Czech forests in 2019, mainly from spruce wood infested with bark beetles (Hlásny et al. 2021). This infestation is primarily caused by higher temperatures and lower precipitation levels (Hlásny et al. 2021). The bark beetle, which is a member of the Scolytinae family, is the most damaging pest for Picea abies (L.) (Schroeder et al. 2018). Despite being small, ranging from two to seven millimeters in size, it can cause multiple stages of infestation by residing under the bark of spruce trees. Therefore, it is imperative to understand the spatial and temporal patterns of bark beetle infestations to limit their spread and consequences. The bark beetle infestation can be classified into 4 stages based on the condition of the tree: 1) *the green stage* where the tree crowns remain green without showing any signs of infestation, 2) *the yellow stage* when the leaves of the tree may turn yellow and eventually brown, indicating that the tree is under severe stress, 3) *the red stage* when the leaves of the tree turn red, indicating that the tree is dying. The bark beetle population is at its highest during this stage, and the tree may be beyond recovery, and finally 4) *the grey stage* where the tree has died, the needles or leaves turned grey and fall off (Bárta et al. 2021). Detecting bark beetle infestations in the green stage is essential for managing and controlling their impact since they pose a considerable threat to Norway spruce trees, resulting in significant harm and loss of trees. The green attack stage refers in the literature to the early stage of bark beetle infestation in which the beetles have penetrated the bark of a tree and started to lay eggs, but visible symptoms of infestation are not yet apparent (Abdullah et al. 2018). It is hypothesized that at this stage, the tree still appears healthy and green, but it could potentially display subtle alterations in its spectral response that might be detected through various remote sensing imaging techniques (Zabihi et al. 2021). To assess the condition of trees infested by bark beetles, many research studies have employed remote sensing datasets, such as Landsat, MODIS, and high-resolution imaging. Some medium-resolution techniques have been successful in the past in detecting and mapping the later stages of infestation (red and grey stages) (Cornelius Senf et al. 2017; Benjamin C. Bright et al. 2014; Nathalie Guimarães et al. 2020). Nevertheless, the detection of early bark beetle infestations (in the green attack stage) requires very high-resolution imagery that can capture the subtle changes of the spectral information on the level of individual trees. Thus, using submeter spatial resolution imagery is crucial (Minařík et al. 2020).

This contribution has been peer-reviewed. The double-blind peer-review was conducted on the basis of the full paper.
https://doi.org/10.5194/isprs-annals-X-1-W1-2023-1033-2023 | © Author(s) 2023. CC BY 4.0 License.

Unmanned aerial vehicles (UAVs) are becoming increasingly important in many applications, and offer a range of benefits, due to their efficiency, flying capacity at low altitudes, and high temporal resolution. These cost-effective devices, equipped with various sensors including RGB, multispectral (MS), and hyperspectral cameras, and offering very high-resolution images, have been widely used in the field of forestry to monitor forest health and detect bark beetle attacks with high accuracy, in the red and grey stages (Junttila et al. 2022, Näsi et al. 2015, Einzmann et al. 2021). This is crucial in assessing economic losses caused by the insects. However, it is not sufficient to prevent the spread of the infestation to other trees in the area. Particularly, MS UAV images were used in the literature and proved their effectiveness in identifying and classifying trees in later stages and dead trees (Minařík et al. 2021, Klouček et al. 2019), and also for the mapping of the later infestation stages during the swarming period (Junttila et al. 2022). Despite that, the detection of the early green attacks using multispectral UAV imagery was still unachievable and has not been conclusively confirmed in the literature. One of the main reasons could be that the detection relied on acquiring either monotemporal or distinct date images (representing different infestation stages), which takes a relatively long time span and is not frequently captured during the green stage before reaching the red and grey attack stages. To date, there has only been one study that utilized time series of MS UAV imagery prior to the attacks, with high temporal resolution (Huo et al. 2023). The images were captured on a weekly basis during the months of May, June, August, and October, in a controlled experiment (Pheromone bags were used to attract bark beetles). Huo et al. (2023) established an approach using the Vegetation Index (VI) in the range of 5-95%, as a criterion for identifying a healthy tree and considered any VI value outside the indicated range as an infested tree. Using detection rates, they conclude that spectral data can detect infestations prior to crown discoloration. However, the early detection of infestations was still not possible in June (1 month after the swarming) (Huo et al. 2023). To detect the infested trees, some studies relied on the visual assessment of the status of the trees in the initial and final orthomosaics using retrospective analysis (Klouček et al. 2019). However, to confirm the results of the spectral variability analysis, it is crucial to collect detailed field data together with remote sensing data sets. Thus far, there is no clear evidence to support the detection of green attacks using multitemporal MS UAV images in previous studies. It is important to examine more thoroughly the use of multi-temporal MS UAV images, to assess the spectral differences between healthy and infested trees before any visible symptoms become apparent on the trees due to the bark beetle attacks in the field, and to investigate the various factors that could influence the spectra before and after swarming. Our study is original as it uses a dense time series of UAV MS data (9 dates) and seeks to examine the green attack stage of bark beetle infestation in the field, before the onset of any observable symptoms on the bark of the trees, and also intensively throughout the swarming period. The approach is supported by ground field data, and by rigorous efforts (during processing) to eliminate potential factors that may impact the spectra of infested trees early in the season.

Considering that, we investigate in this study the potential of multi-temporal MS UAV imagery for early detection of bark beetle infestations in spruce forests. The objective is to explore the specific detection timeframe at which infested trees exhibited an abnormal spectral response compared to healthy trees and to evaluate factors that could influence the detectability of green attacks/early stage of infestation from MS UAV imagery.

2. METHODOLOGY AND EXPERIMENTAL DESIGN

2.1. Area of interest

Our study focuses on a forest in the Krkonoše Mountains National Park (KRNAP), the Czech Republic. The Krkonoše Mountains are the highest mountain range in the country (area of the Krkonoše Mts. is 639 km² (Czech side 454 km², Polish side 185 km²) with the highest mountain Sněžka (1 603 m above sea level). An altitude of area of interest is 1025 m a.s.l. Climate in the mountains is humid, cool and highly variable, with average annual temperature + 6 to 0°C, 800-1 600 mm precipitation per year, 150-300 cm of snow, up to 180 days of snow on the ridges. The Krkonoše Mts. is one of the most important centers of geodiversity in the Czech Republic. Their exceptional location in the middle of European lowlands and hills has allowed the natural evolution of an extraordinarily diverse mosaic of alpine and northern relief. 80% of the territory is covered by forests dominated by Norway Spruce (Picea abies (L.) Karst.). Relict arctic-alpine tundra, peatlands, and wildflower-reach alpine meadows belong among other valuable ecosystems with high biodiversity (including endemic species and glacial relicts). The study area (see Figure 1) covers around 4 hectares of forests dominated by Norway Spruce (Picea abies (L.) H. Karst) in the village of Dolní Dvůr (near the Tetřeví boudy) within the Hradec Králové Region, about 10 kilometers southeast of Vrchlabí city.

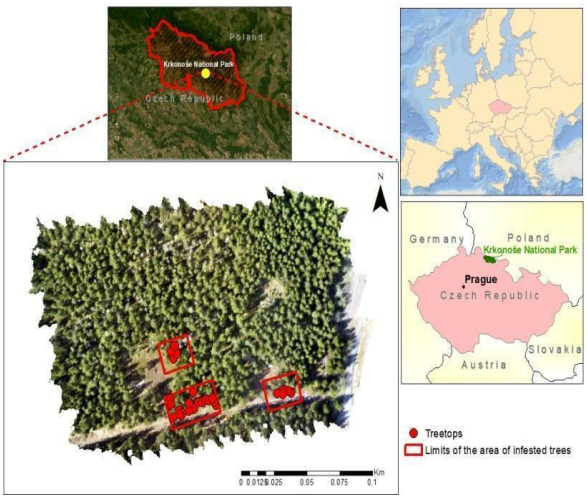

Figure 1. The location of the study area, the RGB Orthomosaic (in the middle) with the location of the infested trees in the subplots

2.2. Field data collection (Imagery and ground truth)

The UAV imagery was acquired before and during the swarming period on nine dates (between May 15th and August 25th, 2022 – see Table 1) with the DJI Phantom 4 Multispectral RTK, equipped with an integrated spectral sunlight sensor that enables capturing solar irradiance and

thus, enhancing the precision and consistency of data collection at different times of the day (Figure. 2). The drone provides images in 5 single bands: blue, green, red, red edge, near-infrared (Table.2) and is also equipped with an RGB camera of a higher spatial resolution.

(a)

(b)

Figure 2. The image of the drone in the field (a), the sensor, and the sunlight sensor (b) (Phantom 4 Multispectral - DJI website)

Ground control points (GCPs) were also used to evaluate the RTK accuracy. The drone was flown at an altitude of 56.9 meters above the ground with 80% overlap in both forward and side directions resulting in an extremely high spatial resolution of 2 cm and during clear weather conditions between 10:26 am and 15:20 pm on all acquisition dates. In our study area, three subplots were the target for bark beetle attacks (Figure.1). With the help of foresters from KRNAP, the collection of ground truth data started on the first day of imagery acquisition in late spring, to identify various infestation symptoms. The ground truth data is important to understand the transition of the tree from a healthy stage to an infested stage, as evidenced by a change in the number of trees throughout the acquisition dates, which can be a reliable indicator of the dynamic processes of this bark beetle disease in the study area. We visually assessed symptoms of infestation by examining holes and resin flow on the bark of the trees in the area of interest. Over time, other symptoms became visible on the trees, with an increase in crown discoloration and defoliation. The location of infested trees was determined in the field using a total station Trimble C5, measuring their X and Y coordinates. Throughout the imagery acquisition period (between mid-May and the end of August), the number of infested trees increased, reaching a total of 36 trees. Some infested trees developed visible symptoms – both on bark and color change of crown needles during the season, while a part that was also infested did not show any visible crown color symptoms.

Date	Time	Number of infested trees
16-may	15:20 pm	0
03-june	11.50.am	10
08-june	11:27.am	13
15-June	12.12.pm	23
24-june	11.18 am	32
01-july	10.53 am	35
19-july	12.40 pm	36
04-august	10.26 am	36
25-august	13.22 pm	36

Table 1. An overview of flight date, time acquisitions and number of infested trees, along with UAV images of an infested tree on the flight dates

Band Number	Band Name	Centre of the wavelength (nm)
1	Blue	450 ± 16 nm
2	Green	560 ± 16 nm
3	Red	650 ± 16 nm
4	RedEdge	730 ± 16 nm
5	NIR	840 ±26 nm

Table 2. Characteristics of the sensor on the Phantom 4 Multispectral

2.3. Data pre-processing workflow

The entire analysis process is illustrated in Figure 3. All RGB and multispectral images acquired underwent the same pre-processing steps. We used Agisoft Metashape Professional v 1.7.2 software (www.agisoft.com, Agisoft LLC, St. Petersburg, Russia) for data georeferencing/alignment and mosaicking. The data processing workflow in Agisoft consists of the following steps: alignment of each image location, generation of dense point cloud (3D-model), creation of Digital Surface Model (DSM), and production of a georeferenced orthomosaics (Iglhaut, Jakob, et al. 2019). The RGB images were utilized for reconstructing the geometry and producing the derived products (DSM), while multispectral images provided spectral information in 5 bands for the extraction of crown symptoms. To radiometrically correct the multispectral images, an additional step was required to remove relatively the differences in weather and seasonal conditions in each UAV sensing period. Thus, we performed a flat field correction in ENVI v5.5 software by using a calibration target (as a flat area), that was placed in the field and was visible on the image at different periods. To accurately determine the position of each infested tree, a local maxima filtering was conducted using the DSM to identify the maxima or peaks. In the applied method, the DSM is first filtered to smooth the image. Then a filter is applied to the image that compares the pixel values in a small neighbourhood around each pixel to find the maximum value (Larsen et al.2011). The filter returns the value of the maximum pixel representing the treetops as shown in Figure 4. Each generated treetop was validated with the measured coordinates of the trees. To mask the understory and shadowed pixels in our orthomosaics, we created two distinct masks, namely the shadow and elevation mask, employing the thresholding approach. The DSM was used to produce the elevation mask, removing the background and understory from the imagery. The NIR band was then used to eliminate shadowed areas from the images. Ultimately, a Boolean raster of the combined two masks constituted the final mask in Figure 4. The manual delineation of trees was performed in ArcGIS Version 10.8.1 (Esri, 2021), encompassing all pixels within the tree crown while excluding shadowed branches and mixed pixels, to achieve a precise identification of tree crowns. The statistics for the five individual single bands and Normalized Difference Vegetation Index (NDVI) were extracted for each date to the manually delineated trees (Mean, Max, Min, standard deviation). All the extracted information was organized in data frames for further processing and analysis.

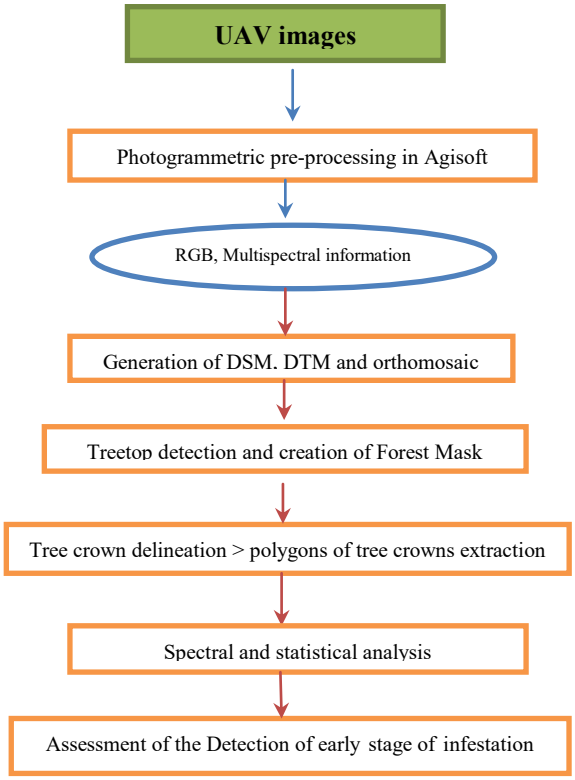

Figure 3. The workflow adopted in our study

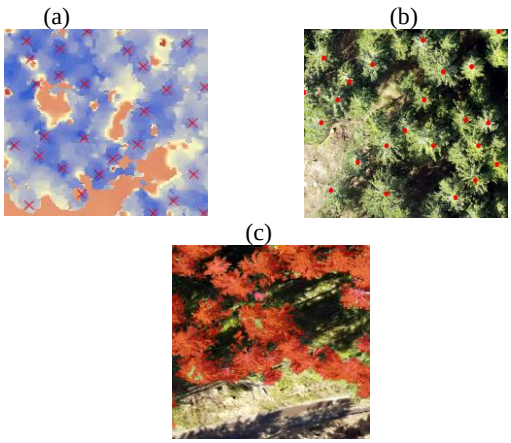

Figure 4. Results of Automatic treetop detection on DSM and RGB orthomosaic (a, b), and Forest Mask (c)

2.4. Spectral and statistical analysis

This study sought to determine in which date the spectral features (single bands or NDVI) of infested trees pronounced a change to spectral features of the healthy trees. Prior to conducting the statistical analysis, the spectral profiles of each infested tree were examined. The temporal spectral analysis was carried out independently for each acquisition date, utilizing below described statistical methods. Due to the absence of absolute reflectance calibration, relative reflectance between infested and healthy trees was analyzed as independent samples. For the statistical analysis, a typical sample of 20 infested trees out of 36 was selected, as some of the trees exhibited partly some dead branches due to drought stress (not related to bark beetle infestation), and trees that did not develop visible symptoms had to be discarded. All trees were assumed to be in the green stage during the initial acquisition date, and consequently, were considered infested, despite variations in their individual infestation timelines in the field, owing to the lack of precision and clarity regarding the green stage period. As a result, our analysis centered on two primary categories of data, namely trees that were infested (20 trees) and those that were healthy (20 trees for each time period). To extract the spectral information of healthy trees from the images, the mean reflectance was used and was based on two criteria: the first one is to be at a considerable distance from the subplots of infested trees ($\simeq$ 20 meters buffer) and the second is to extract the trees, showing a clear healthy status of the tree crown. All spectral data (mean spectral reflectance and mean NDVI) was tested for normality using the Shapiro-Wilk test. Consequently, to determine the separability between the 2 groups (Healthy and Infested), either a t-test (in case of normality of the data) or a Wilcoxon rank-sum test (lack of normality) was conducted to assess the significance between the healthy and infested trees. A variance analysis with a p-value of 0.01 was used to compare the spectra of the 2 classes and identify the sensitive spectral bands or features to the infestation in different time periods.

3. RESULTS AND DISCUSSION

3.1. Temporal change of infested trees:

Initially, there were 10 infested trees in the field on 3rd June, but their number gradually increased and peaked in early July (1st July) - see Table 1 and Figure 5. In all dates of the MS data acquisition, the study area was checked for new infested trees. The first indications of infestation were holes and flow resin (first noticed on the 3rd of June), followed by yellow needles and discoloration. The initial observable symptoms at the crown level were observed on July 1st when some leaves and branches started to turn yellow, because of the loss of their chlorophyll content.

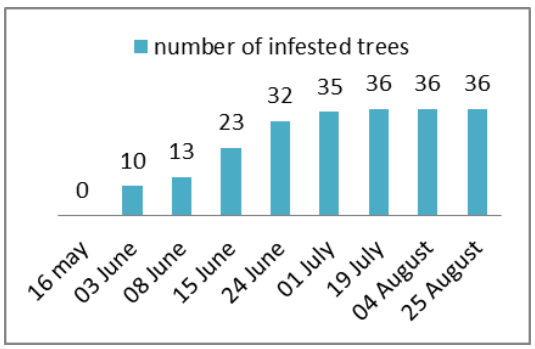

Figure 5. Temporal change in the detection of newly infested trees in the field

3.2. Analysis of Spectral Variability

The reflectance values for the infested and healthy trees were analyzed for each of the five single spectral bands to observe their variation and the extracted values were used to draw the spectral reflectance curve for each date. The results of spectral analysis of the infested trees including spectral signatures and comparison of NDVI between healthy and infested samples are shown in Figure

6 and Figure 7 (see appendices). For the study, we analyzed the data based on three intervals (according to the season and the development of the attack in the field): the first interval (15 May to the end of June 24) comprised five dates, the second interval consisted of two dates in July (1st and 19th of July), and the third interval encompassed two dates in August (04th and 25th of August). Results from temporal comparison of the first-period interval including spectral signatures and p-values (>0.01) indicated that the spectral response of the infested trees in comparison to the healthy trees displayed atypical characteristics of the bark beetle infestation, suggesting that early variations in spectral response during the June swarming were not a reliable indicator of an infestation (as the p-values increased in the second period interval). However, the relative comparison between healthy and infested trees for this first interval, on each date, showed fluctual changes in the spectra and separability between the 2 classes of healthy and infested, particularly on the 3rd and 6th of June, where the two groups of trees exhibited lower p-values for the NDVI comparing to p-values of the other dates. We consider the flowering and the appearance of new shoots as one of the reasons of fluctuation in this first period interval.

During the progression of the bark beetle attack in the second time interval, the temperatures were higher but there was no separability between the 2 classes in the spectra in the 5 bands and NDVI, resulting in high p-values (>0.01) on 1st of July compared to 19th of July, where the 2 classes started to exhibit separability with p-values (<0.01) in the NIR and Rededge parts of the spectrum.

A spectral variation was evident and visible during the third period (starting on the 4th of August) when the difference in the range of the spectral response of healthy and infested trees was detected in the Red, Rededge, and NIR parts of the spectrum. The spectral bands that were observed showed notable changes between the 2 classes. By August 4th, the reflectance levels for the infested trees became higher in the red band, while lower in the NIR, in comparison to the healthy trees, with p-values <0.01. However, no significant changes were observed in other parts of the spectrum (Green band). The spectral reflectance on the last date indicated that the trees had died, resulting in higher reflectance in the visible part of the spectrum and lower in the NIR. The values of NDVI were also compared and displayed in boxplots (Figure.7), where it was observed that the two samples were highly distinguishable starting from August 4th.

Multi-temporal analysis involves comparing UAV data at different times, and reflectance values can significantly vary over time due to several factors. When trees undergo stress, they produce compounds such as phenolics and terpenes that may affect the spectral signature of the tree, making it more sensitive to changes (Martin et al. 2003). During the first time interval (mid-May to the end of June particularly on June 3rd and 6th), we noticed that the spectral differences between healthy and infested trees were fluctuating which may be due to various factors (rather than just bark beetle infestation). In general, one of the most likely factors that could be responsible for the spectral change between the 2 classes could be the variations in atmospheric conditions within the orthomosaics, which can affect the amount of sunlight reaching the tree crown and lead to differences in reflectance values. In order to reduce this issue, the statistical analyses were conducted using independent samples based on relative reflectance for each date. Despite attempting to change the combination of the spectra of healthy samples, there was no improvement in the results during the initial first interval. Additionally, the shadowing of some tree crowns can cast shadows on other parts of the crown, resulting in variations in reflectance values. To overcome this, shadowed pixels of the tree crowns were eradicated in our study during the precise manual delineation. By conducting image acquisitions under clear weather conditions on specific days, the impact of weather conditions also on the spectral differences between the two classes was mitigated. On the 3rd of June, the first trees were infested, and the spruce bloom occurred. In the spring (from April to June), new growth or pollen on the branches of spruce trees may create a visual effect that is sometimes referred to as a bloom or a haze. The possible outcome of the blooming of spruce trees may result in a decreasing effect in chlorophyll manifestation in the spectra of the flowering branches, making them appear less green than the non-flowering branches, resulting in a higher level of light being reflected by the flowering branches, which have a lower capacity to absorb visible light. As a result, the flowering branches have a higher reflectance in the visible compared to the non-flowering ones. The flowering on the 3rd and 6th of June could be the reason of the low reflectance in the NIR and differences in p-values (lower NDVI p-values) between dates in the first period Table.3 (see appendices). However, it is important to investigate furthermore in future studies the effects of flowering on infested and healthy trees and examine if there is a difference in the reaction of these 2 groups to the flowering of spruce trees.

The results indicate that the most accurate detection of tree vitality using multispectral images occurs at the end of summer (the end of July and the beginning of August), which is consistent with the research conducted by Samuli Junttila et al. in 2022. Their study aimed to map the decline of trees caused by the European spruce bark beetle infestation in four regions of Helsinki, Finland. During the months of May and September, the imagery was acquired in 2 days. They found that the end of summer or fall (September) was the optimal period for obtaining precise classification outcomes for tree vitality. Additionally, the outcomes of our study are compliant with the conclusions reached by Klouček et al. 2019 regarding the effectiveness of RGB and multispectral images in accurately detecting changes in the same region of the Krkonoše Mountains. They were able to observe modifications in vegetation indices, between healthy and infested trees later in the season, during their second acquisition date (August 1st), with a significant detection mainly in the Red band. The study conducted by Huo et al. in 2023, used dense time series of multispectral data. Even though there were differences in the sensor and the area studied in comparison with our study, neither was successful in detecting statistically significant changes in the spectral characteristics of trees due to the swarming early in May and June.

In our study, we investigated the possibility of the detection of bark beetle attack in MS data with very high spatial resolution using dense time series of images from UAV prior to the infestation, during the initial and later stages of infestation. Covering the whole season by the imagery we were able to detect the date and bands showing the first significant changes in the spectra between healthy

and infested trees. Detailed field work and field data collection showed the peculiarities of the development of bark beetle infestation. The evolution in the field, where groups of trees were attacked successively from 3 June to the first of July, meant that there were trees in different stages of infestation, which could have influenced the result. The question is whether in studies of larger spatial extent, where not all trees in the stand are monitored in detail, only two phases of bark beetle swarming actually occur or whether the number of infested trees also increases outside these more pronounced phases. This should be verified in detail in future studies as it can influence the results of the analysis. While we were able to demonstrate that distinguishing between healthy and infested trees becomes more feasible over time, particularly in the Red, RedEdge, and NIR parts of the spectrum in the middle of summer, we were unable to identify any subtle changes or separability that would allow us to differentiate between the two groups during the green stage (end of spring/early summer). Our results can also be affected by the size of the sample of infested trees. All these above-mentioned factors were eliminated as far as possible in our study using independent statistical testing for each date and the comparison of different combinations of the sample trees. Namely, the results showed that there was no improvement in the detectability of the green attack using multispectral imagery despite the use of very high spatial resolution images, the accurate pre-processing methods including precise generation of forest mask and relative radiometric correction (based on precise visual interpretation and the choice of the green pixels with uniform lighting conditions), and different combinations of independent samples of the healthy trees (used in the comparison using the statistical test).

As shown in other studies (Minařík et al. 2021, Minařík et al. 2020, Junttila et al. 2022), multispectral sensors that have fewer spectral bands may not be able to detect early subtle changes in reflectance caused by bark beetle infestations. This can lead to inaccuracy in the detection of infested trees during the green attack stage. However, the finer spectral resolution (more narrow bands) of hyperspectral imagery is typically better for more precise identification and characterization of the spectral signature of the infested trees, which may provide a more detailed and nuanced picture of the green stage detection. Some studies investigated the efficiency of bark beetle infestation using UAV hyperspectral imagery, achieving good results for the classification of the different stages (Näsi et al. 2015). Different trees in different infestation stages of stress can exhibit unique spectral signatures. By analysing these spectral profiles of healthy and infested trees, hyperspectral images can detect the specific wavelengths at which changes in reflectance occur and the early signs of green attack that might not be discernible to the human eye. This capability allows for proactive interventions before the damage becomes severe. Our study confirms that determining the precise time of infestation in the green attack stage using UAV multispectral images remains a difficult task.

4. CONCLUSION

UAVs are gaining importance in forest health assessment and monitoring, due to the numerous benefits they offer (high spatial and temporal resolution). Our study investigated the potential of UAV Multispectral imagery with very high spatial (2 cm) and temporal (9 dates) resolution for the detection of bark beetle green attack. We acquired images prior to infestation and during the infestation that caused tree damage and we also tried to determine the spectral bands that exhibited noteworthy variations in spectra between healthy and infested trees. Our findings demonstrate the potential of multispectral data for the detection of spruce forest damage due to bark beetle infestations, particularly in the late summer season. The analysis of the multi-date UAV multispectral image revealed a clear decline in tree health of the infested trees starting from the 4th of August. The use of UAVs equipped with multispectral sensors can provide reliable information on changes in forest health and the vitality of trees, in later stages of infestations (red and grey attack), particularly with changes in the Red, Rededge, and NIR parts of the spectrum. However, our research findings imply that the detection of the "green attack" phase of infestation from multispectral imagery remains difficult even using dense time series of images and precise pre-processing and processing methods.

ACKNOWLEDGEMENTS

We want to thank for the support to the Technology Agency of the Czech Republic (project SS05010124 Assessment of the impact of land cover changes on local hydrology and climate in the Krkonoše Mts. National Park using remote sensing and hydrological modelling).

REFERENCES

Bright, B.C., Hudak, A.T., Kennedy, R.E., Meddens, A.J.H., 2014. Landsat time series and lidar as predictors of live and dead basal area across five bark beetle-Affected forests. IEEE J. Sel. Top. Appl. Earth Obs. Remote Sens. 7, 3440–3452.

ABDULLAH, Haidi, Roshanak DARVISHZADEH, Andrew K. SKIDMORE, Thomas A. GROEN a Marco HEURICH. European spruce bark beetle (Ips typographus, L.) green attack affects foliar reflectance and biochemical properties. International Journal of Applied Earth Observation and Geoinformation. 2018, 64, 199-209 [cit. 2020-06-04]. DOI: 10.1016/j.jag.2017.09.009. ISSN 03032434

Einzmann, Kathrin, Clement Atzberger, Nicole Pinnel, Christina Glas, Sebastian Böck, Rudolf Seitz, and Markus Immitzer. 2021. “Early Detection of Spruce Vitality Loss with Hyperspectral Data: Results of an Experimental Study in Bavaria, Germany.” Remote Sensing of Environment 266(May). doi: 10.1016/j.rse.2021.112676.

Hlásny, T., S. Zimová, K. Merganičová, P. Štěpánek, R. Modlinger, and M. Turčáni. 2021. “Devastating Outbreak of Bark Beetles in the Czech Republic: Drivers, Impacts, and Management Implications.” Forest Ecology and Management 490:119075. doi: 10.1016/j.foreco.2021.119075.

Huo, Langning, Eva Lindberg, Jonas Bohlin, and Henrik Jan Persson. 2023. “Assessing the Detectability of European Spruce Bark Beetle Green Attack in Multispectral Drone Images with High Spatial- and Temporal Resolutions.” Remote Sensing of Environment 287(February):113484. doi: 10.1016/j.rse.2023.113484.

Iglhaut, Jakob, Carlos Cabo, Stefano Puliti, Livia Piermattei, James O’Connor, and Jacqueline Rosette. 2019. “Structure from Motion Photogrammetry in Forestry: A

Review." Current Forestry Reports 5(3):155–68. doi: 10.1007/s40725-019-00094-3.

Junttila, Samuli, Roope Näsi, Niko Koivumäki, Mohammad Imangholiloo, Ninni Saarinen, Juha Raisio, Markus Holopainen, Hannu Hyyppä, Juha Hyyppä, Päivi Lyytikäinen-Saarenmaa, Mikko Vastaranta, and Eija Honkavaara. 2022. "Multispectral Imagery Provides Benefits for Mapping Spruce Tree Decline Due to Bark Beetle Infestation When Acquired Late in the Season." Remote Sensing 14(4). doi: 10.3390/rs14040909.

Klouček, Tomáš, Jan Komárek, Peter Surový, Karel Hrach, Přemysl Janata, and Bedřich Vašíček. 2019. "The Use of UAV Mounted Sensors for Precise Detection of Bark Beetle Infestation." Remote Sensing 11(13):1–17. doi: 10.3390/rs11131561.

Larsen, Morten, Mats Eriksson, Xavier Descombes, Guillaume Perrin, Tomas Brandtberg, and François A. Gougeon. 2011. "Comparison of Six Individual Tree Crown Detection Algorithms Evaluated under Varying Forest Conditions." International Journal of Remote Sensing 32(20):5827–52. doi: 10.1080/01431161.2010.507790.

Minařík, Robert, Jakub Langhammer, and Theodora Lendzioch. 2020. "Automatic Tree Crown Extraction from Uas Multispectral Imagery for the Detection of Bark Beetle Disturbance in Mixed Forests." Remote Sensing 12(24):1–31. doi: 10.3390/rs12244081.

Minařík, Robert, Jakub Langhammer, and Theodora Lendzioch. 2021. "Detection of Bark Beetle Disturbance at Tree Level Using Uas Multispectral Imagery and Deep Learning." Remote Sensing 13(23). doi: 10.3390/rs13234768.

Näsi, Roope, Eija Honkavaara, Päivi Lyytikäinen-Saarenmaa, Minna Blomqvist, Paula Litkey, Teemu Hakala, Niko Viljanen, Tuula Kantola, Topi Tanhuanpää, and Markus Holopainen. 2015. "Using UAV-Based Photogrammetry and Hyperspectral Imaging for Mapping Bark Beetle Damage at Tree-Level." Remote Sensing 7(11):15467–93. doi: 10.3390/rs71115467.

Nathalie Guimarães , Luís Pádua, Pedro Marques , Nuno Silva, Emanuel Peres and Joaquim J. Sousa. Forestry Remote Sensing from Unmanned Aerial Vehicles: A Review Focusing on the Data, Processing and Potentialities, Remote Sens. 2020, p 12.

Schroeder, Martin, and Dragoş Cocoş. 2018. "Performance of the Tree-Killing Bark Beetles Ips Typographus and PityogenesChalcographus in Non-Indigenous Lodgepole Pine and Their Historical Host Norway Spruce." Agricultural and Forest Entomology 20(3):347–57. doi: 10.1111/afe.12267.

Bárta, Vojtěch, Petr Lukeš, and Lucie Homolová. 2021. "Early Detection of Bark Beetle Infestation in Norway Spruce Forests of Central Europe Using Sentinel-2." International Journal of Applied Earth Observation and Geoinformation 100:102335. doi: 10.1016/j.jag.2021.102335.

Senf, Cornelius, Dirk Pflugmacher, Patrick Hostert, and Rupert Seidl. 2017. "Using Landsat Time Series for Characterizing Forest Disturbance Dynamics in the Coupled Human and Natural Systems of Central Europe." ISPRS Journal of Photogrammetry and Remote Sensing 130:453–63. doi: 10.1016/j.isprsjprs.2017.07.004.

Zabihi, Khodabakhsh, Peter Surovy, Aleksei Trubin, Vivek Vikram Singh, and Rastislav Jakuš. 2021. "A Review of Major Factors Influencing the Accuracy of Mapping Green-Attack Stage of Bark Beetle Infestations Using Satellite Imagery: Prospects to Avoid Data Redundancy." Remote Sensing Applications: Society and Environment 24(May). doi: 10.1016/j.rsase.2021.100638.

Martin, D. M., Gershenzon, J. and Bohlmann, J. 2003. Induction of volatile terpene biosynthesis and diurnal emission by methyl jasmonate in foliage of Norway spruce. Plant Physiol., 132, 1586-99.

Agisoft Metashape Professionnal v 1.7.2 software (www.agisoft.com, Agisoft LLC, St. Petersburg, Russia)

https://www.dji.com/cz/p4-multispectral

APPENDICES

Date	P-values (NDVI)
16/05	0.6316
03/06	0.05225
08/06	0.05618
15/06	0.4881
24/06	0.4488
01/07	0.7272
19/07	0.1597
04/08	0.002341
25/08	0.007544

Table 3. Results of the statistical tests (p-values) to distinguish between healthy and infested trees for each date of acquisition. The light blue indicates that the result of the statistical test show significant changes with p-values ~ 0.05 and the light orange indicates highly significant separability with p-values < 0.01. The light green indicates no separability between the infested and healthy trees

Figure 8. UAV picture of an infested tree during the entire sensing period

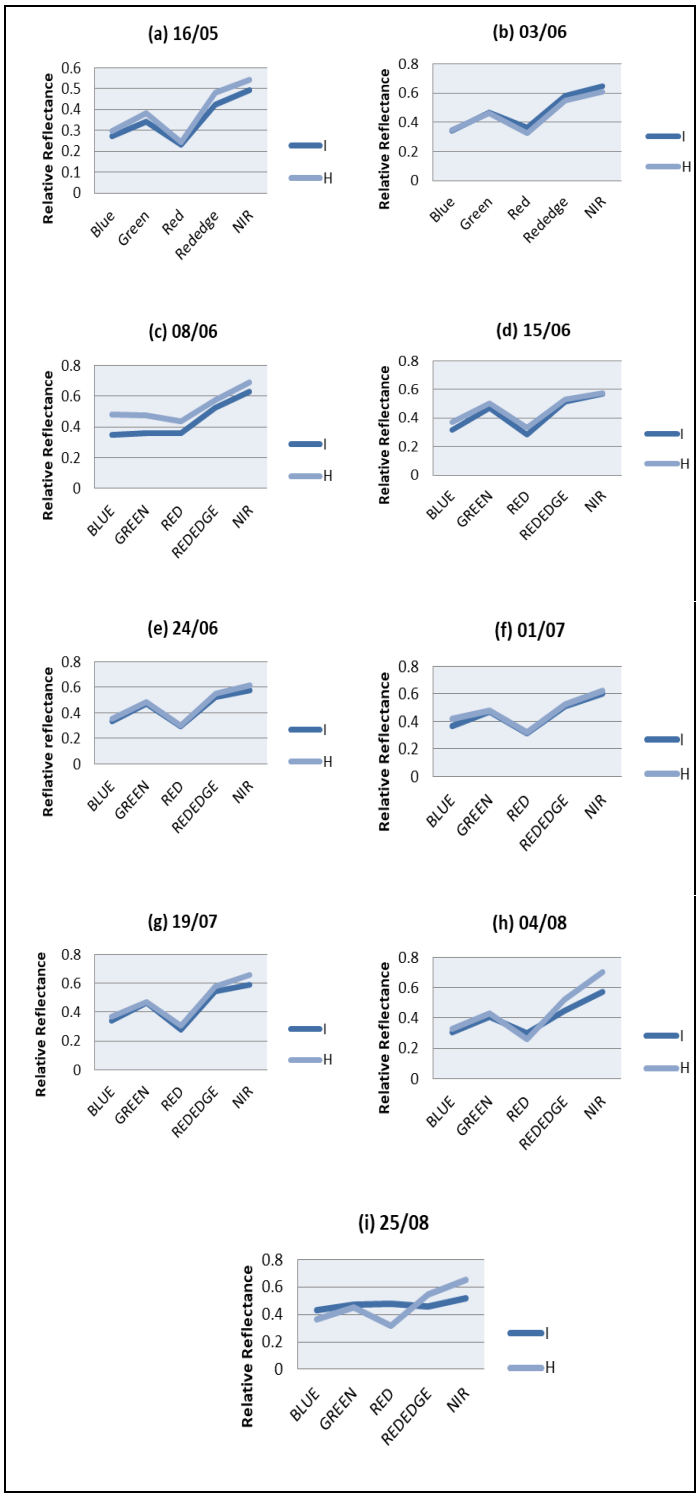

Figure 6. Spectral profiles of the 2 samples healthy (H) and infested (I) for each date of acquisition in 2022 (a). 16 May, (b), 03 June, (c). 08 June, (d). 15 June, (e). 24 June,(f). 01 July, (g).19 July, (h).04 August, (i).25 August (I: Infested Trees, H: Healthy trees)

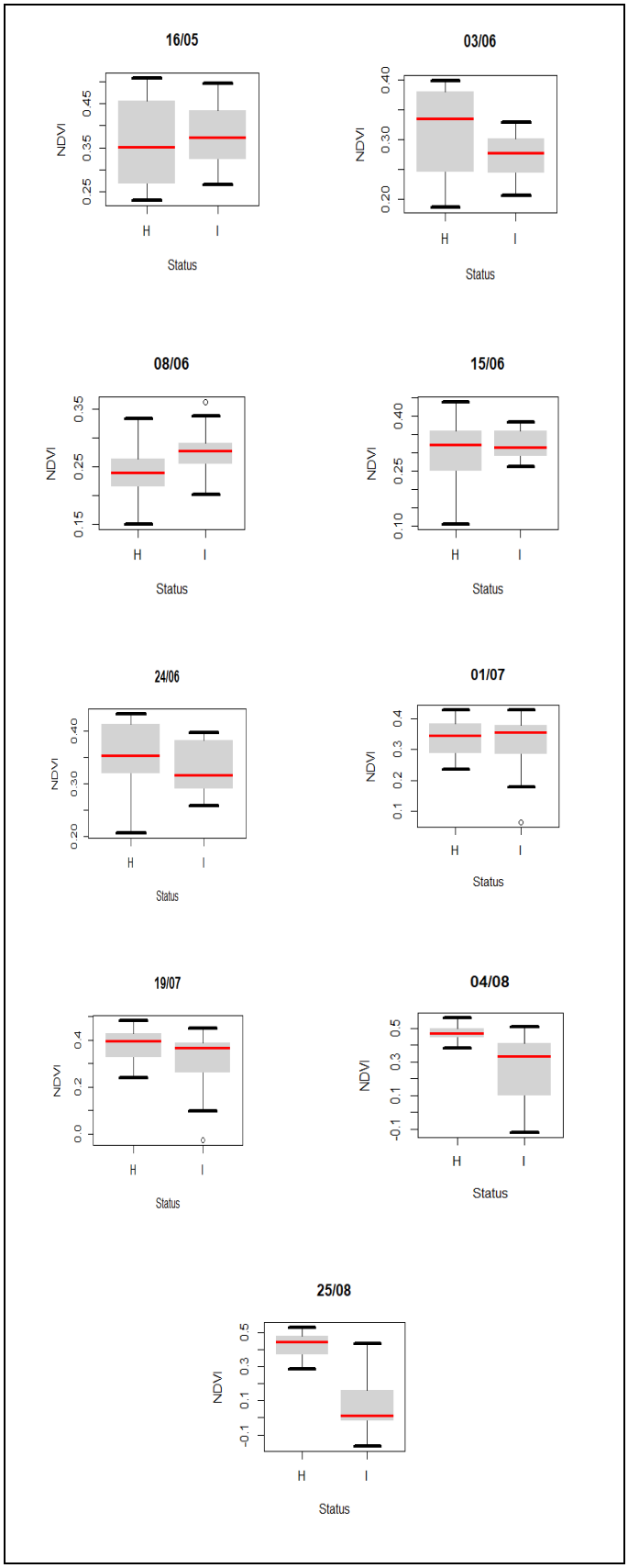

Figure 7. Boxplots of NDVI for the 2 samples healthy (H) and infested (I) for each date of acquisition in 2022 (a). 16 May, (b), 03 June, (c). 08 June,(d). 15 June,(e). 24 June, (f). 01 July, (g).19 July, (h).04 August, (i).25 August (I: Infested Trees, H: Healthy trees)